Diffusive Transport across Corrugated Plates and Tubes

The steady diffusion across a constant thickness corrugated barrier is analyzed through the intrinsic coordinate system. Perturbation solutions are found when the thickness is small compared to the minimum radius of curvature. For a given perimeter length, diffusive transfer is decreased, while for given maximum geometric dimensions, diffusive transfer may be increased by corrugations.

C.-Y. WANG

Department of Mathematics
Michigan State University
East Lansing, MI 48824

SCOPE

Steady diffusion of heat, mass, or concentration across a barrier is important in many chemical engineering processes. If the barrier has linear material properties, the distribution of the diffuser (heat, mass or concentration) is governed by Laplace's equation. An analytic solution can be found if the boundary of the barrier falls into any one of the *separable* orthogonal coordinate systems. (Morse and Feshbach 1953, Crank 1956.) The present paper investigates the diffusion across corrugated plates and tubes, which are becoming more important due to their resistance to bending. Corrugated boundaries can only be described by an intrinsic, *nonseparable* coordinate system. Instead of the traditional separation of variables, we use perturbation theory to study the diffusion properties.

CONCLUSIONS AND SIGNIFICANCE

The steady concentration distribution across a barrier for the case of periodic centerline curvature is now determined. It is found that the mean curvature of a thin barrier always increases the concentration within the material of the barrier. On the other hand, the corrugations increase the concentration in segments convex to the source of the diffuser. For the same perimeter length, although net diffusive transfer is slightly decreased by the corrugations, the maximum dimensions may be greatly decreased. Thus, corrugated plates and tubes are attractive not only due to their resistance to bending, but also due to possible increased net transfer for given maximum geometric dimensions.

FORMULATION

Figure 1 shows the cross-section of a corrugated plate which cannot be described by any of the conventional coordinate systems. The only way to solve this problem is to use an intrinsic coordinate system to describe the geometry.

The Frenet formulas are

$$T = \frac{dR}{ds'}, \qquad \frac{dT}{ds'} = K'N, \qquad \frac{dN}{ds'} = -K'T \tag{1}$$

where $K'(s')$ is the curvature. Any point inside the plate is described by

$$x' = R(s') + \eta' N(s') + z'k \tag{2}$$

The equation $\eta' = \pm d$ describes the boundary of the plate. Using Eqs. 1 and 2, the elemental length is

$$|dx'|^2 = (1 - K'\eta')^2(ds')^2 + (d\eta')^2 + (dz')^2 \tag{3}$$

We write the diffusion equation in intrinsic coordinates:

$$\frac{\partial T'}{\partial t'} = \frac{D}{(1-K'\eta')}\left\{\frac{\partial}{\partial s'}\left[\frac{1}{(1-K'\eta')}\frac{\partial T'}{\partial s'}\right] + \frac{\partial}{\partial \eta'}\left[(1-K'\eta')\frac{\partial T'}{\partial \eta'}\right] + \frac{\partial}{\partial z'}\left[(1-K'\eta')\frac{\partial T'}{\partial z'}\right]\right\} \tag{4}$$

For two-dimensional steady diffusion, Eq. 4 reduces to the nonseparable Laplace equation:

$$\frac{\partial}{\partial s'}\left[\frac{1}{(1-K'\eta')}\frac{\partial T'}{\partial s'}\right] + \frac{\partial}{\partial \eta'}\left[(1-K'\eta')\frac{\partial T'}{\partial \eta'}\right] = 0 \tag{5}$$

Assuming homogeneous "well mixed" conditions on both sides of the plate, the boundary conditions are

$$T' = T_i \text{ on } \eta' = -d, \qquad T' = T_e \text{ on } \eta = +d \tag{6}$$

PERIODIC CURVATURE

We shall concentrate on corrugated plates or cylinders whose centerline curvatures are described by

$$K' = a' + b' \cos \lambda' s', \tag{7}$$

To find the coordinates (x', y') of this centerline, one solves

$$\frac{d\theta}{ds'} = K'(s'), \qquad \frac{dx'}{ds'} = \cos\theta, \qquad \frac{dy'}{ds'} = \sin\theta, \tag{8}$$

When $a' = 0$, we can normalize all lengths by $1/b'$:

$$\tilde{K} \equiv K'/b', \qquad \tilde{s} \equiv s'b', \qquad \tilde{\lambda} = \lambda'/b'$$
$$\tilde{x} \equiv x'b', \qquad \tilde{y} \equiv y'b' \tag{9}$$

Then

$$\frac{d\theta}{d\tilde{s}} = \cos\tilde{\lambda}\tilde{s}, \qquad \frac{d\tilde{x}}{d\tilde{s}} = \cos\theta, \qquad \frac{d\tilde{y}}{d\tilde{s}} = \sin\theta \tag{10}$$

The configurations for $a' = 0$ are shown in Figure 2. In order to avoid cross-over of the centerline, $\tilde{\lambda}$ should be larger than 0.472.

When $a' \neq 0$ we similarly normalize all lengths by $1/a'$. The result is

$$\frac{d\theta}{d\tilde{s}} = 1 + \beta \cos\tilde{\lambda}\tilde{s} \tag{11}$$

0001-1541-82-6220-1016-$2.00.

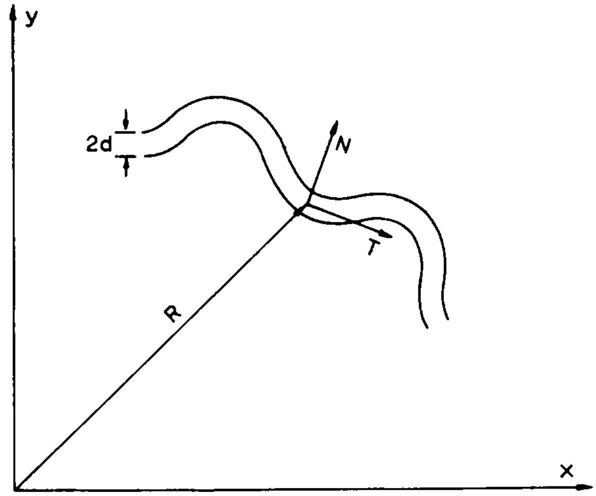

Figure 1. The intrinsic coordinate system.

$$\frac{d\tilde{x}}{d\tilde{s}} = \cos\theta, \qquad \frac{d\tilde{y}}{d\tilde{s}} = \sin\theta, \tag{12}$$

Of interest are the centerline configurations which represent corrugated tubes with N fold symmetry. Let the total perimeter length be $\tilde{s}^*$. From Eq. 11, we conclude

$$\tilde{\lambda}\tilde{s}^* = 2\pi N \tag{13}$$

Integrating Eq. 11 and substituting into Eq. 12 yield

$$\frac{d\tilde{x}}{d\tilde{s}} = \cos\left[\tilde{s} + \frac{\beta}{\tilde{\lambda}}\sin(\tilde{\lambda}\tilde{s})\right], \qquad \frac{d\tilde{y}}{d\tilde{s}} = \sin\left[\tilde{s} + \frac{\beta}{\tilde{\lambda}}\sin(\tilde{\lambda}\tilde{s})\right] \tag{14}$$

Since for closed tubes $\tilde{x},\tilde{y}$ is once periodic in $[0,\tilde{s}^*]$, Eq. 14 gives

$$\tilde{s}^* = 2\pi \tag{15}$$

Eqs. 13 and 15 gives the condition on frequency $\tilde{\lambda}$

$$\tilde{\lambda} = N \tag{16}$$

Thus

$$\frac{d\tilde{x}}{d\tilde{s}} = \cos\left[\tilde{s} + \frac{\beta}{N}\sin(N\tilde{s})\right], \qquad \frac{d\tilde{y}}{d\tilde{s}} = \sin\left[\tilde{s} + \frac{\beta}{N}\sin(N\tilde{s})\right] \tag{17}$$

The actual total perimeter length is $2\pi/a'$, independent of N and β. Equation 17 is integrated numerically and the results are shown in Figure 3. We see that a wide variety of shapes is represented. The geometries are convex when $\beta \leq 1$.

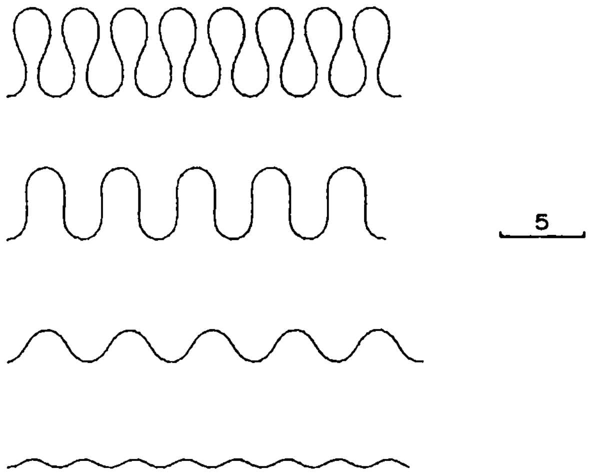

Figure 2. Centerline configurations for $a' = 0$. The value of $\tilde{\lambda}$ from top to bottom is 0.5, 0.6, 1,2.

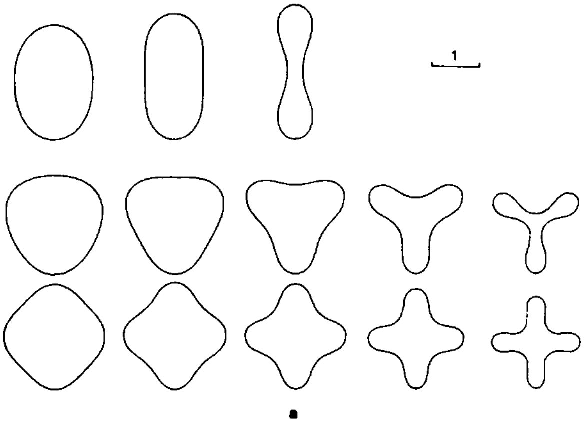

Figure 3a. Centerline configurations for $a' \neq 0$.

Top row: $N = 2, \beta = 0.5$, 1,2; middle row: $N = 3, \beta = 0.5$, 1, 2, 3, 4; bottom row: $N = 4, \beta = 1$, 2, 3, 4, 5.

PERTURBATION SOLUTION WHEN THE THICKNESS IS SMALL COMPARED TO THE RADIUS OF THE CURVATURE

Although the boundary representation is much simplified by our intrinsic coordinate system, Eq. 5 is unseparable. We renormalize our variables as follows.

$$\eta \equiv \eta'/d, \qquad s \equiv s'/d, \qquad K \equiv K'd$$
$$T \equiv \frac{T' - T_e}{T_i - T_e} \tag{18}$$

Equation 5 becomes

$$\frac{\partial}{\partial s}\left[\frac{1}{(1 - K\eta)}\frac{\partial T}{\partial s}\right] + \frac{\partial}{\partial \eta}\left[(1 - K\eta)\frac{\partial T}{\partial \eta}\right] = 0 \tag{19}$$

$$T(s,-1) = 1 \qquad T(s,1) = 0 \tag{20}$$

Analytic perturbation solutions of Eqs. 19 and 20 are possible if the half thickness d is small compared to the radius of curvature $1/K'$. We define a small number ϵ such that

$$K \equiv \epsilon k(s) \ll 1, \tag{21}$$

where $k(s)$ is of order unity. Set

$$T = T_0(s,\eta) + \epsilon T_1(s,\eta) + \epsilon^2 T_2(s,\eta) + \ldots \tag{22}$$

The perturbation equations are

$$\frac{\partial^2 T_0}{\partial s^2} + \frac{\partial^2 T_0}{\partial \eta^2} = 0, \qquad T_0(s,-1) = 1, \qquad T_0(s,1) = 0 \tag{23}$$

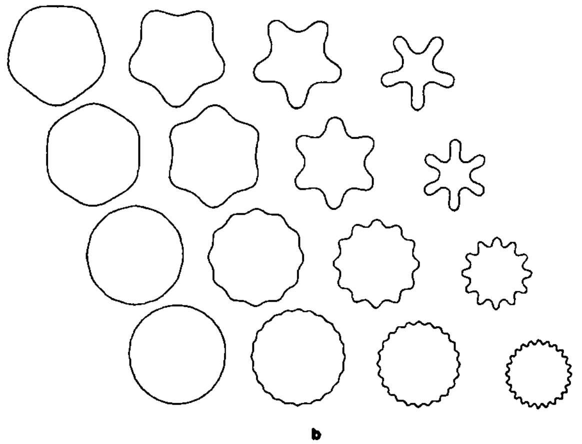

Figure 3b. Centerline configurations for $a' \neq 0$.

Top row: $N = 5, \beta = 1$, 3, 5, 7; second row: $N = 6, \beta = 1$, 3, 6, 9; third row: $N = 12, \beta = 1$, 5, 10, 15; bottom row: $N = 24, \beta = 1$, 10, 20, 30.

$$\frac{\partial^2 T_1}{\partial s^2} + \frac{\partial^2 T_1}{\partial \eta^2} = -\frac{\partial}{\partial s}\left(k\eta\frac{\partial T_0}{\partial s}\right) + \frac{\partial}{\partial \eta}\left(k\eta\frac{\partial T_0}{\partial \eta}\right), \quad T_1(s,\pm 1) = 0 \tag{24}$$

$$\frac{\partial^2 T_2}{\partial s^2} + \frac{\partial^2 T_2}{\partial \eta^2} = -\frac{\partial}{\partial s}\left(k\eta\frac{\partial T_1}{\partial s} + k^2\eta^2\frac{\partial T_0}{\partial s}\right) + \frac{\partial}{\partial \eta}\left(k\eta\,\frac{\partial T_1}{\partial \eta}\right), \quad T_2(s,\pm 1) = 0 \tag{25}$$

The solution to Eq. 23 is

$$T_0 = \tfrac{1}{2}(1 - \eta) \tag{26}$$

For the case of periodic curvature, Eqs. 7, 18 and 21 give

$$k(s) = a + b\cos\lambda s, \tag{27}$$

where

$$a \equiv a'd/\epsilon = 0(1), \qquad b \equiv b'd/\epsilon = 0(1), \qquad \lambda' = \lambda/d \tag{28}$$

Using Eqs. 24, 26 and 27, we find

$$\frac{\partial^2 T_1}{\partial s^2} + \frac{\partial^2 T_1}{\partial \eta^2} = -\tfrac{1}{2}(a + b\cos\lambda s) \tag{29}$$

The solution is

$$T_1 = f(\eta) + g(\eta)\cos\lambda s, \tag{30}$$

where

$$f(\eta) = \frac{a}{4}(1 - \eta^2), \; g(\eta) = \frac{b}{2\lambda^2}\left(1 - \frac{\cosh\lambda\eta}{\cosh\lambda}\right) \tag{31}$$

Then Eq. 25 becomes

$$\frac{\partial^2 T_2}{\partial s^2} + \frac{\partial^2 T_2}{\partial \eta^2} = \frac{\partial}{\partial s}\left[\lambda\eta g\left(a\sin\lambda s + \frac{b}{2}\sin 2\lambda s\right)\right] + \frac{\partial}{\partial \eta}\left[a\eta f' + (ag' + bf')\eta\cos\lambda s + \frac{b}{2}\eta g'(1 + \cos 2\lambda s)\right] \tag{32}$$

The solution is

$$T_2 = h(\eta) + \ell(\eta)\cos\lambda s + m(\eta)\cos 2\lambda s, \tag{33}$$

where

$$h(\eta) = \frac{a^2}{6}(\eta - \eta^3) + \frac{b^2}{4\lambda^2\cosh\lambda}\left[\frac{\sinh\lambda\eta}{\lambda} - \eta\cosh\lambda\eta + \left(\cosh\lambda - \frac{\sinh\lambda}{\lambda}\right)\eta\right] \tag{34}$$

$$\ell(\eta) = \frac{ab}{2}\left[\frac{\eta}{\lambda^2} - \frac{\eta^2\sinh\lambda\eta}{2\lambda\cosh\lambda} - \left(\frac{1}{\lambda^2\sinh\lambda} - \frac{1}{2\lambda\cosh\lambda}\right)\sinh\lambda\eta\right] \tag{35}$$

$$m(\eta) = \frac{b^2}{4}\left[\frac{-\eta}{2\lambda^2} + \frac{\eta\cosh\lambda\eta}{\lambda^2\cosh\lambda} + \frac{\sinh\lambda\eta}{\lambda^3\cosh\lambda} - \left(\frac{1}{2\lambda^2} + \frac{\tanh\lambda}{\lambda^3}\right)\frac{\sinh 2\lambda\eta}{\sinh 2\lambda}\right] \tag{36}$$

DISCUSSION

Although intrinsic coordinates have been introduced before (e.g., Goldstein, 1938), perturbation solution of the field equations in terms of these coordinates is fairly recent (Wang, 1980). The present paper applies this method to an important diffusion problem for the first time.

For small ϵ, the zeroth order solution, Eq. 26, represents the well-known linear concentration distribution across a flat plate. The first order correction, Eq. 30, consists of a sum of two parts. The s-independent part $f(\eta)$ shows that mean curvature always increase the concentration within the material of the plate. The other part is periodic in λs. Since $g(\eta)$ is always positive, the concentration is increased for the segment of the corrugated plate or cylinder which are convex to the source of the diffuser.

The net diffusive transfer is

$$Q = \int -D\frac{\partial T'}{\partial \eta'}(1 - K'\eta')ds' \tag{37}$$

If we integrate for N periods on $\eta' = d$, Eq. 37 becomes

$$\frac{Q}{D(T_i - T_e)} = -N\int_{-\pi/\lambda}^{\pi/\lambda}\left.\frac{\partial T}{\partial \eta}\right|_1(1 - \epsilon k)ds = -\frac{2\pi N}{\lambda}\left\{-\tfrac{1}{2} + \epsilon^2\left[h'(1) - af'(1) - \frac{b}{2}g'(1)\right] + 0(\epsilon^4)\right\} \tag{38}$$

From Eq. 38 we conclude

$$\frac{Q}{Q_s} = 1 - \epsilon^2 G(\lambda,a,b) + 0(\epsilon^4), \tag{39}$$

where

$$G(\lambda,a,b) = \frac{a^2}{3} + \frac{b^2}{2\lambda^2}\left(1 - \frac{\tanh\lambda}{\lambda}\right), \tag{40}$$

and Q_s is the transfer when the plate is flat; i.e., $\epsilon = 0$. Since $G > 0$, the corrugations always decrease diffusive transfer for a given perimeter length of the plate. To relate to dimensional parameters, we recall when $a' = 0$, $b = 1$ or $\epsilon = b'd$ and $\lambda = \lambda'd = \tilde{\lambda}\epsilon$. When $a' \neq 0$ we set $a = 1$ or $\epsilon = a'd$. Then $b = b'/a' = \beta$ and $\lambda = \lambda'd = \tilde{\lambda}\epsilon$.

The function G for $a = 0$ is plotted in Figure 4. Note that $G \rightarrow 1/6$ when $\lambda \rightarrow 0$ and $G \rightarrow 1/(2\lambda^2)$ when $\lambda \rightarrow \infty$. Equation 39 shows the more pronounced the corrugations (decrease in λ), the less the net transfer for a given minimum radius of curvature.

Figure 5 shows the function $G(\lambda)$ for $a = 1$ and various b or β. G increases with increased b and decreased λ. Now the cylindrical forms shown in Figure 3 have the same perimeter length $2\pi/a'$. For fixed thickness d, λ is directly proportional to the number of

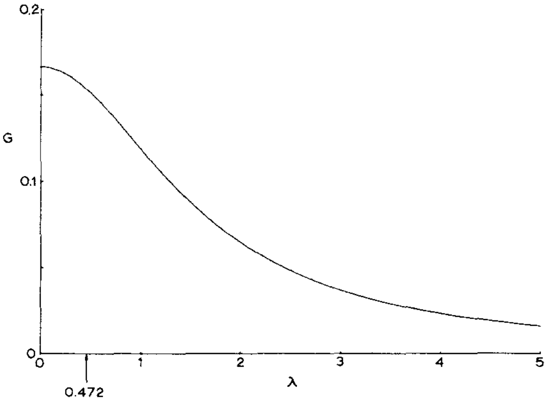

Figure 4. The function $G(\lambda)$ for $a = 0$, $b = 1$.

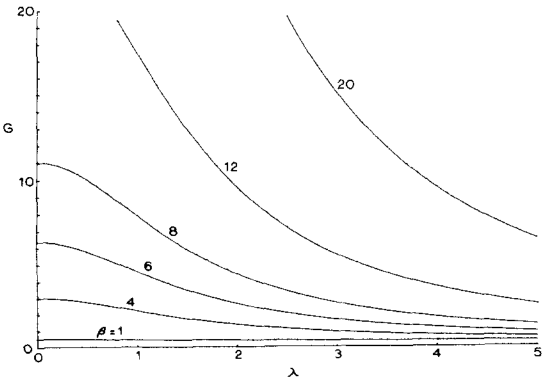

Figure 5. The function $G(\lambda)$ for $a = 1$ and various b.

periods N. Thus, the net transfer decreases for both a *decrease* in N and an increase in amplitude b.

Our results show net diffusive transfer is somewhat decreased (proportional to ϵ^2) by corrugations if the *perimeter length is fixed.* However, from Figure 3 we see that corrugations may also cause a large reduction in the maximum dimensions. Thus, for *given maximum dimensions*, although the net transfer is decreased by corrugations, this decrease may be more than offset by a concurrent increase in perimeter length. This is exemplified by the microvilli in the digestive tract and hollow core cooling fins on heat engines. We must keep in mind that corrugations may not automatically increase net transfer for given maximum dimensions. There may be cases where large ϵ, λ, a or b cause such a decrease in net transfer that cannot be compensated by the concurrent increase in perimeter length. One must make a careful calculation using the results of this paper.

Since our perturbation Eq. 23–25 are linear in k, our present method may be extended to any periodic curvature

$$k = a + \sum b_n \cos\lambda ns. \quad (41)$$

Lastly, the present analysis can be applied to various kinds of diffusive transfer other than the flow of heat, mass or concentration. One example is the electric potential distribution inside corrugated capacitor plates. Another instance is the $\mathbf{k}$ direction parallel motion of corrugated plates separated by a viscous fluid. Both problems are governed by Eqs. 5 and 6.

NOTATION

a = mean curvature
b = amplitude of corrugation
d = ½ thickness
D = diffusion coefficient
f,g,h = functions of s,η
G = function of λ,a,b
k = scaled curvature
$\mathbf{k}$ = unit vector in z direction
K = curvature
ℓ,m = functions of η
n = integer
N = N-fold symmetry
$\mathbf{N}$ = unit normal
Q = net transfer
$\mathbf{R}$ = position vector of centerline
s = arc length
$\mathbf{T}$ = unit tanget
T = concentration of diffuser
$\mathbf{x}$ = position of vector
x,y,z = Cartesian coordinates

Greek Letters

β = b'/a'
ϵ = small number
η = normal coordinate
θ = local angle of inclination of centerline
λ = frequency of corrugation

Superscripts

= dimensional quantity
= quantity renormalized with respect to b'

LITERATURE CITED

Crank, J., *The Mathematics of Diffusion*, Clarendon Press, Oxford (1956).
Goldstein, S., *Modern Developments in Fluid Dynamics*, **1**, Clarendon Press, Oxford, 119 (1938).
Morse, P. M., and H. Feshbach, *Methods of Theoretical Physics*, **1**, McGraw-Hill, New York (1953).
Wang, C.-Y., "Flow in Narrow Curved Channels," *J. Appl. Mech.* **47**, 7–10 (1980).

Manuscript received August 4, 1981; revision received October 19, and accepted November 5, 1981.

Model of Solid Gas Reaction Phenomena in The Fluidized Bed Freeboard

L. H. CHEN and C. Y. WEN

Department of Chemical Engineering
West Virginia University
Morgantown, WV 26506

A comprehensive model incorporating elutriation, entrainment and reaction is presented to describe the chemical reaction and hydrodynamics occurring in the freeboard of a fluidized bed. A comparison of experimental data on the amount of particles elutriated and the concentration profiles of SO_2 and NO_x obtained from the freeboard of fluidized bed coal combustion (FBC) by the Babcock & Wilcox Company with the calculation based on the proposed model to include the effect of interaction among the entrained particles is desirable. More experimental data with chemical reactions in the freeboard are needed to validate the model for applications to fluidized bed catalytic reactors.

SCOPE

When bubbles burst at the fluidized bed surface, particles are entrained in the freeboard region. The entrained particles with a terminal velocity greater than the actual gas velocity will reach a certain height within the freeboard before they fall back into the bed. However, those particles with a terminal velocity smaller than the actual gas velocity will be elutriated and carried out of the bed. Because of good solid-gas contact in the

C. Y. Wen is deceased.
0001-1541-82-5468-1019-$2.00.